# The equation of state of two dimensional Yang-Mills theory

Nikhil Karthik* and Rajamani Narayanan†

*Department of Physics, Florida International University, Miami, FL 33199.*

arXiv:1411.2477v1 [hep-th] 10 Nov 2014

## Abstract

We study the pressure, $P$, of SU($N$) gauge theory on a two-dimensional torus as a function of area, $A = l/t$. We find a cross-over scale that separates the system on a large circle from a system on a small circle at any finite temperature. The cross-over scale approaches zero with increasing $N$ and the cross-over becomes a first order transition as $N \to \infty$ and $l \to 0$ with the limiting value of $\frac{2Pl}{(N-1)t}$ depending on the fixed value of $Nl$.

*Electronic address: nkarthik@fiu.edu

†Electronic address: rajamani.narayanan@fiu.edu

## I. INTRODUCTION

The partition function for SU($N$) gauge theory on a 2d torus with spatial extent $l$ and temperature $t$ is only a function of the area, $A = l/t$, and is given by [1]

$$Z_N(A) = \sum_r \exp\left(-\frac{C_r^{(2)} l}{Nt}\right), \tag{1}$$

where $C_r^{(2)}$ is the value of Casimir in the representation $r$. One can arrive at (1) by taking the continuum limit of a lattice formalism on a finite lattice [2]. The asymptotic behavior at large $N$ was studied in [3] where only representations with $C_r^{(2)}$ of $\mathscr{O}(N)$ dominate. Since the partition function is a sum over string like states with energies proportional to the spatial extent, $l$, the pressure given by

$$P \equiv t\frac{\partial}{\partial l}\ln Z = \frac{\partial}{\partial A}\ln Z = -\frac{1}{N}\langle C_r^{(2)}\rangle, \tag{2}$$

is negative.

The partition function for SU(2) is simple and given by

$$Z = \sum_{\lambda=0}^{\infty} e^{-\frac{\left(\lambda^2+2\lambda\right)A}{4}} = \frac{1}{2}e^{\frac{A}{4}}\left[\sum_{\lambda=-\infty}^{\infty} e^{-\frac{\lambda^2 A}{4}} - 1\right] = \frac{1}{2}e^{\frac{A}{4}}\left[\sqrt{\frac{4\pi}{A}}\sum_{\lambda=-\infty}^{\infty} e^{-\frac{4\pi^2\lambda^2}{A}} - 1\right]. \tag{3}$$

The asymptotic behavior of the equation of state is

$$\frac{Pl}{t} = -\frac{3}{4}\frac{l}{t}e^{-\frac{3l}{4t}} \quad \text{as} \quad l \to \infty, \tag{4}$$

and

$$\frac{Pl}{t} = -\frac{1}{2} \quad \text{as} \quad l \to 0. \tag{5}$$

The behavior at large $l$ is dominated by a few low lying energy states where as the behavior at small $l$ comes from a sum over all states and could be interpreted as the equipartition limit with the number of degrees of freedom being 1 for SU(2). The cross-over from the behavior on a large circle to a small circle is shown in Figure 1.

Expecting that the equipartition limit is given by

$$\frac{Pl}{t} = -\frac{N-1}{2} \quad \text{as} \quad l \to 0, \tag{6}$$

for all $N$, we define

$$Q(\alpha) \equiv -\frac{2Pl}{(N-1)t}; \quad \text{with} \quad \alpha = \frac{Nl}{t}, \tag{7}$$

and study this quantity in this paper.

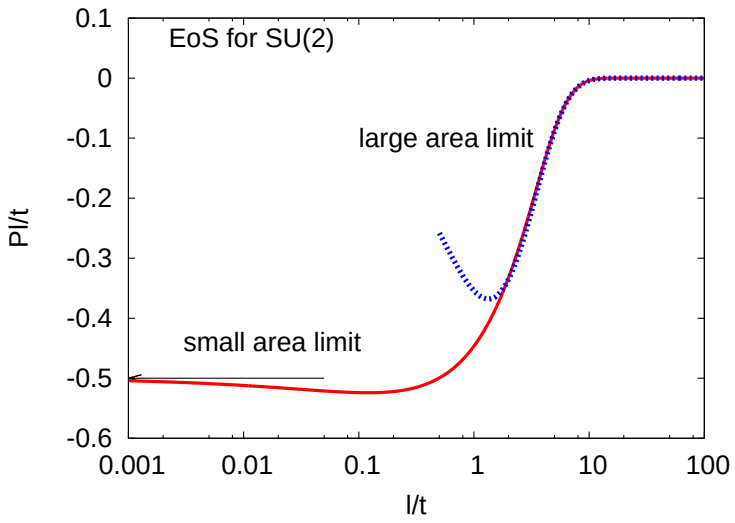


FIG. 1: The equation of state for SU(2) gauge theory on a two-dimensional torus is shown as the solid curve. The asymptotic values of $Pl/t$ at small area is -0.5. At very large area, $Pl/t$ behaves as $0.75\exp(-0.75l/t)l/t$, which is shown as the dotted curve. There is a cross-over between the two limits.

## II. SUMMARY OF RESULTS

We will show the following results in this paper using a numerical simulation of the partition function in Eq. (1):

1. $Q(\alpha)$ falls on a universal curve as $N \to \infty$.

2. $Q(\alpha)$ goes to zero as $\alpha$ goes to infinity. This result implies that the pressure at infinite $N$ is zero for all $l$ at any $t$ as long as one takes $N \to \infty$ keeping $l$ and $t$ finite and is consistent with physics being independent of temperature and spatial extent in the infinite $N$ limit [4, 5].

3. $Q(\alpha)$ goes to unity as $\alpha$ goes to zero. This limit is reached from a finite $l$ and $t$ only at finite $N$.

4. There is a cross-over point defined as a peak in the susceptibility,

$$\chi = A\frac{\partial}{\partial A}Q = \alpha\frac{\partial}{\partial \alpha}Q. \tag{8}$$

(a) The large $l$ side of the cross-over is dominated by representations where $C_r^{(2)}$ are of $\mathscr{O}(N)$. This is the case of interest for all non-zero $l$ at infinite $N$ and studied in [3].

(b) The small $l$ side of the cross-over is dominated by representations where $C_r^{(2)}$ are of $\mathscr{O}(N^2)$.

5. Since the value of $Q$ at infinite $N$ and $l = 0$ (or equivalently $t = \infty$) depends on the approach to the limit, $N \to \infty$ and $l \to 0$, there is a first order transition confirming the argument in [6].

## III. PROPERTIES OF CASIMIR FOR SU(N)

The representations of SU($N$) are specified by the sequence of integers $\Lambda_r = (\lambda_1, \lambda_2, \ldots, \lambda_{N-1})$, subjected to the ordering $\lambda_i \geq \lambda_{i+1}$ and the value of $C_r^{(2)}$ is

$$C_r^{(2)} = \sum_{i=1}^{N-1} \lambda_i^2 - \sum_{i=1}^{N-1} i\lambda_i - \frac{\lambda^2}{N} + (N+1)\lambda \quad \text{where} \quad \lambda = \sum_{i=1}^{N-1} \lambda_i. \tag{9}$$

The maximum and the minimum value of Casimir, given the constraint that $\lambda$ has to be kept fixed, would be used in the subsequent sections. The representation with the maximum value of $C_r^{(2)}$ for a given $\lambda$ is given by

$$\Lambda_{\max} = (\lambda, 0, \ldots, 0). \tag{10}$$

The minimum value of $C_r^{(2)}$ is given by the sequence $\Lambda_{\min}$:

$$\lambda_i = \begin{cases} \lfloor \frac{\lambda}{N-1} \rfloor + 1 & \text{if } i \leq k \equiv \lambda - (N-1)\lfloor \frac{\lambda}{N-1} \rfloor \\ \lfloor \frac{\lambda}{N-1} \rfloor & \text{if } i > k. \end{cases} \tag{11}$$

To prove that the two sequences extremize the Casimir, note that the Casimir decreases under the transformation $(\lambda_1, \lambda_2, \ldots, \lambda_i, \ldots, \lambda_j, \ldots, \lambda_{N-1})$ to $(\lambda_1, \lambda_2, \ldots, \lambda_i - 1, \ldots, \lambda_j + 1, \ldots, \lambda_{N-1})$ for $j > i$, provided this transformation is allowed. Such a transformation is not possible for $\Lambda_{\min}$. Similarly, the reverse of that transformation is not possible on $\Lambda_{\max}$. One can prove by contradiction that $\Lambda_{\min}$ and $\Lambda_{\max}$ are unique to satisfy these properties.

We have shown the behaviour of the maximum and the minimum value of $C_r^{(2)}$ as a function of $\lambda$ in Figure 2. The minimum of $C_r^{(2)}$ shows a quasi-periodic behaviour, with

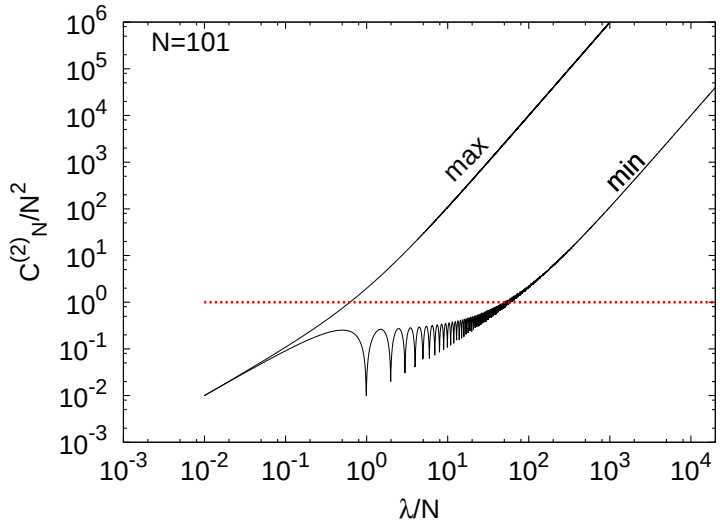


FIG. 2: Behaviour of Casimir as a function of $\lambda$. The upper solid curve is the maximum value of Casimir given a value of $\lambda$, as a function of $\lambda$. Similarly, the lower solid curve is the minimum value of Casimir given a value of $\lambda$, as a function of $\lambda$. The dotted line is where $C_r^{(2)} = N^2$.

troughs at $\lambda = qN$ for integer $q$. The values of Casimir at these troughs are

$$C_{\min} = N\left(1 + \left\lfloor \frac{q}{N-1} \right\rfloor\right)\left(2q - \left\lfloor \frac{q}{N-1} \right\rfloor (N-1)\right), \tag{12}$$

whose dependence on $N$ is linear for $q$ between two multiples of $(N-1)$ and is quadratic for $q$ that are multiples of $(N-1)$. On very large circles (or at very low temperatures), one would expect that only the excitations around these troughs at small $q$ would be important. On very small circles (or at very high temperatures), large values of $q$ would become accessible, where all possible Casimir are $\mathscr{O}(N^2)$. This is the region above the red dotted line in Figure 2 where $C_r^{(2)}$ is larger than $N^2$. Qualitatively, this is the difference one might expect between the low and high temperature phases.

## IV. HEAT-BATH ALGORITHM

We simulated the partition function in Eq. (1) by updating $\Lambda_r$ by the heat-bath algorithm. Each heat-bath update is a sequence of local updates from $\lambda_1$ to $\lambda_{N-1}$, in that order, such that the ordering of $\lambda_i$ is preserved. For the local update of $\lambda_i$, the probability distribution

of $\lambda_i$ is given by a discrete version of the Gaussian distribution

$$T(\lambda_i) \propto e^{-(\lambda_i-\mu_i)^2/2\sigma^2}, \tag{13}$$

subject to the condition $\lambda_{i+1} \leq \lambda_i \leq \lambda_{i-1}$ for $i > 1$ and $\lambda_2 \leq \lambda_1$. The $\mu_i$ and $\sigma_i$ for the above discrete Gaussian distribution are functions of the rest of the $\lambda_i$'s forming the heat-bath:

$$\mu_i = \frac{\overline{\lambda} + N\left(\frac{2i-N-1}{2}\right)}{N-1} \quad \text{and} \quad \sigma^2 = \frac{N^2}{2A(N-1)}, \tag{14}$$

where $\overline{\lambda} = \sum_{j\neq i} \lambda_j$. For $i > 1$, the set of allowed values for $\lambda_i$ is bounded from above and below. Hence, we included all the allowed possibilities weighted by Eq. (13) as candidates for the update. Since Eq. (14), along with the inequality $\lambda - \lambda_1 < (N-2)\lambda_2$, implies that $\mu_1 < \lambda_2$, the probability for $\lambda_1$ is a monotonically decreasing function. This enables one to put an upper cut-off on $\lambda_1$. In our calculation, we used an upper cut-off of $\lambda_2 + 3\sigma$. We also checked that changing this value to $\lambda_2 + 10\sigma$ does not cause any statistically significant changes. Since a representation $r$ and its conjugate representation $\overline{r}$ have the same Casimir, one can do an over-relaxation step by a global update $\lambda_i' = \lambda_1 - \lambda_{N-i+1}$.

In our simulations, the successive measurements were separated by 100 iterations of 2 heat-bath and 1 over-relaxation steps. The first 2000 measurements were discarded for thermalization. In this way, we collected $10^4$ configurations of $\Lambda_r$ at all area and $N$.

## V. RESULTS

In the top panel of Figure 3, we show the behaviour of $Q$ as a function of the scaled area $\alpha$ for various values of $N$. The important thing to notice is that $Q$ has a large-$N$ limit when plotted as a function of $\alpha$. For $\alpha \ll 1$, $Q$ seems to approach 1 for all $N$. This is in agreement with our intuition based on the equipartition theorem. The non-trivial observation is that this cross-over to the equipartition limit happens at a finite value of $\alpha$ in the large-$N$ limit. For $\alpha \gg 1$, $Q$ seems to behave as $N^{-1}\exp(-\sigma\alpha/N)$ for a constant $\sigma \approx 0.81$ in the large-$N$ limit. This is shown in the bottom panel of Figure 3. Thus, it can also be seen as a cross-over from strong-coupling regime, which has a scale $\sigma$, to the weak-coupling regime with no underlying scale.

We determined the cross-over point $\alpha_c$ using the peak-position of the susceptibility $\chi$, after interpolating using multi-histogram reweighting. We show $\chi$ as a function of $\alpha$ in

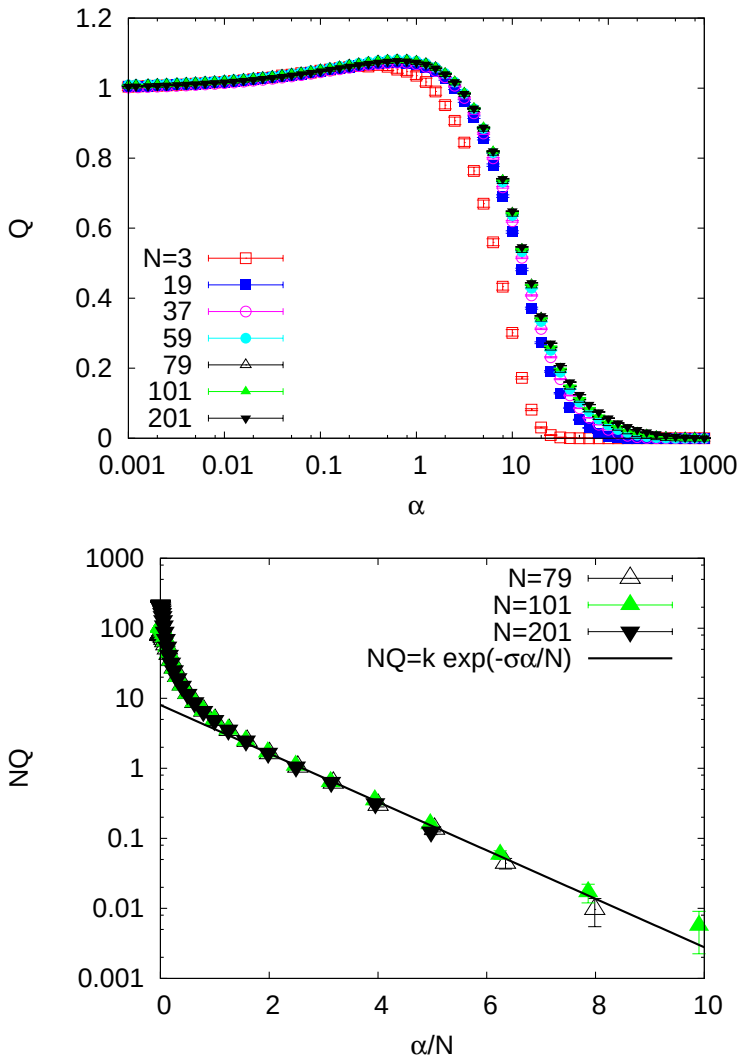


FIG. 3: $Q$ as a function of the scaled area $\alpha = NA$ is shown in the top panel. It is seen that $Q$ as a function of $\alpha$ has a large-$N$ limit. For very small values of $\alpha$, $Q$ approaches 1. In the bottom panel, the large area behaviour of $Q$ in the large-$N$ limit is shown. In this case, $QN$ behaves as $\exp(-\sigma\alpha/N)$.

Figure 4 for various $N$. The susceptibility also has a large-$N$ limit when plotted as a function of $\alpha$. The peak positions of susceptibility for $N > 19$ agree within errors, giving us an estimate $\alpha_c = 12.1(2)$. This implies that the cross-over area $A_c = \alpha_c/N$ shifts to smaller values at larger $N$. The width of the susceptibility when expressed in terms of the area $A$ decreases inversely as $N$. This is characteristic of finite volume scaling near a first order phase transition, with the large-$N$ limit replacing the thermodynamic limit in this case.

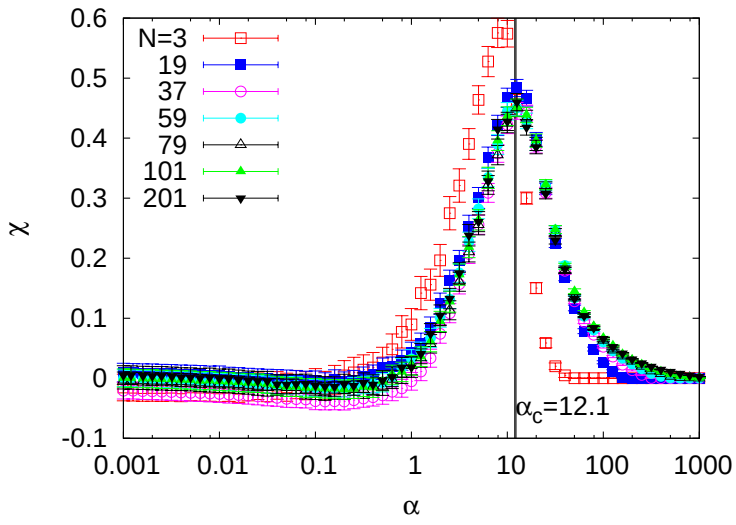


FIG. 4: Susceptibility $\chi$ as a function of the scaled area $\alpha = NA$. The cross-over coupling $\alpha_c$ is shown by the vertical line.

The reason for this cross-over can be understood from the scatter plot of $C_r^{(2)}$ versus $\lambda$ measured during the course of the Monte Carlo run using a value of $\alpha$. Such scatter plots at various $\alpha$ are shown in Figure 5 for two different $N$. We also show the maximum and minimum value of Casimir at a fixed $\lambda$, as a function of $\lambda$. As discussed earlier, the minimum Casimir shows a quasi-periodic behaviour forming wells with a periodicity $N$. At large values of $\alpha$, the representations near the troughs of these wells at small values of $\lambda$ get populated. The representations within these wells are sparse, and this discreteness govern the large area behaviour. At very small area, the most probable $C_r^{(2)}$ moves away from the line of minimum $C_r^{(2)}$ and remains in a region where one can approximate the distribution of Casimir by a continuum. The cross-over between the two behaviours is what shows up as a peak in $\chi$. As discussed in Section III, the Casimir near the troughs at small $\lambda$ is of $\mathscr{O}(N)$, while the Casimir at very large $\lambda$ is of $\mathscr{O}(N^2)$. As shown by the dotted line in Figure 5, this cross-over at $\alpha \approx 12.1$ roughly occurs when the dominant behaviour $C_r^{(2)}$ changes from $\mathscr{O}(N)$ to $\mathscr{O}(N^2)$.

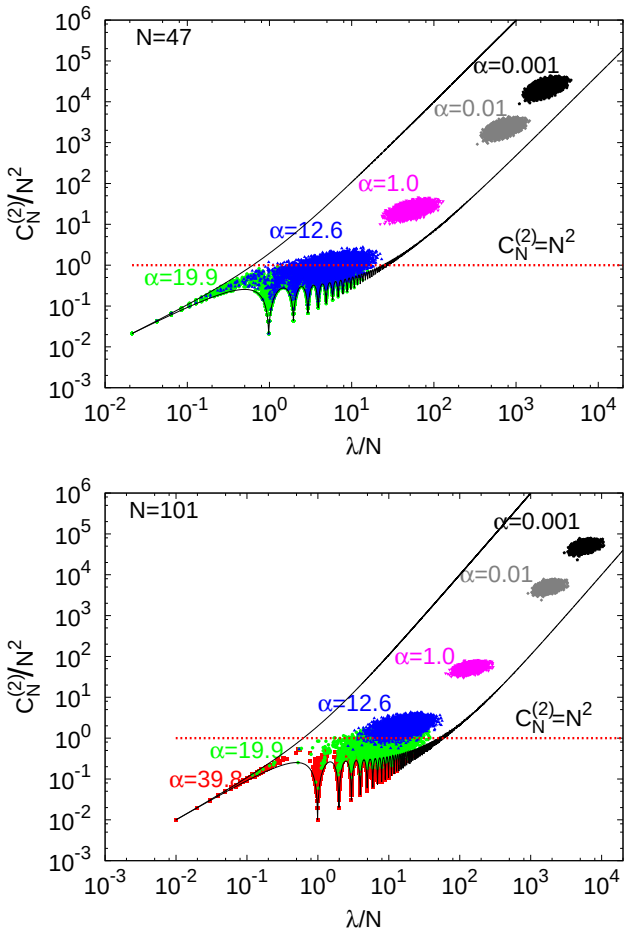


FIG. 5: Scatter plot of $C_r^{(2)}/N^2$ versus $\lambda/N$ at various area $A$. The top panel is for $N = 47$ and the bottom one for $N = 101$. Each point corresponds to a $C_r^{(2)}$ and $\lambda$ measured in the course of Monte Carlo simulation at a particular $\alpha$ specified by the color. The upper and lower solid curves are the maximum and the minimum value of $C_r^{(2)}$ at a given $\lambda$ respectively.

## VI. CONCLUSIONS

Yang-Mills theory in two dimensions is always in the confined phase. We focused on the quantity, $Q = -\frac{2Pl}{(N-1)t}$, to study the equation of state. We showed that the equation of state shows a cross-over from strong coupling (large spatial extent) to weak coupling (small spatial extent) within the confined phase. Viewed as a function of $\alpha = \frac{lN}{t}$, $Q(\alpha)$ approaches a universal curve as $N \to \infty$ as shown in Figure 6. This behavior is similar to the Durhuus-Olesen transition [7, 8] with the double scaling limit for the equation of state being $N \to \infty$ and $l \to 0$ (or $t \to \infty$) keeping $\alpha = \frac{lN}{t}$ fixed. There is a line of cross-over, $\frac{lN}{t} = \alpha_c$, extending

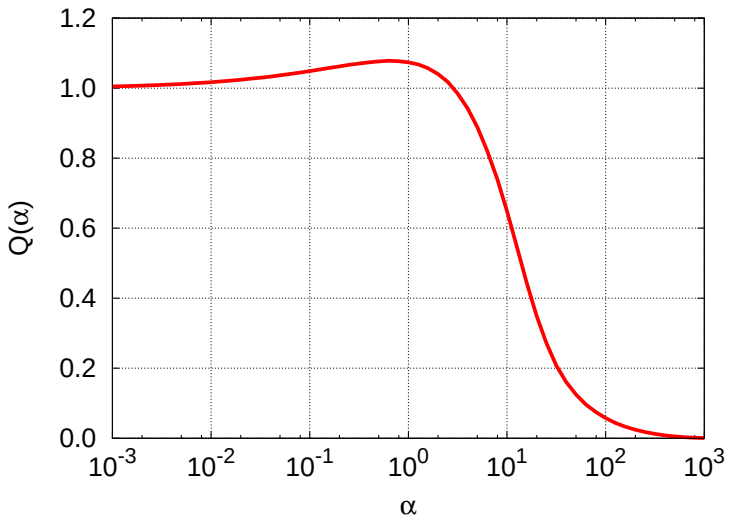


FIG. 6: The large-$N$ limit of $Q$ as a function of $\alpha$.

from the origin in the $\frac{l}{t} - \frac{1}{N}$ diagram as shown in Figure 7. Well above this line, $Q \ll 1$ and it behaves as $\exp(-\sigma A)/N$. Well below this line, $Q$ is approximately 1. Depending on the slope, $\alpha$, of the line along which the $N \to \infty$ and $\frac{l}{t} \to 0$ limit is taken, the limiting value of $Q$ differs. Specifically, if $N \to \infty$ limit is taken after the $A \to 0$ limit is taken, then $Q$ is 1. When the two limits are reversed, $Q$ becomes 0. Therefore, the cross-over along $AN = \alpha_c$ becomes a first order transition at vanishing area in the large-$N$ limit.

The equation of state in four dimensional Yang-Mills theories for several different values of $N$ has been recently studied [9]. The pressure is found to be close to zero in the confined phase. In light of this paper, it would be interesting to perform a careful study of the equation of state in the confined phase in three and four dimensions and see if one can see a cross-over similar to the one seen here in two dimensions.

**Acknowledgments**

The authors acknowledge partial support by the NSF under grant number PHY-1205396.

[1] A. A. Migdal, Sov.Phys.JETP **42**, 413 (1975).

[2] J. Kiskis, R. Narayanan, and D. Sigdel, Phys.Rev. **D89**, 085031 (2014), 1403.1770.

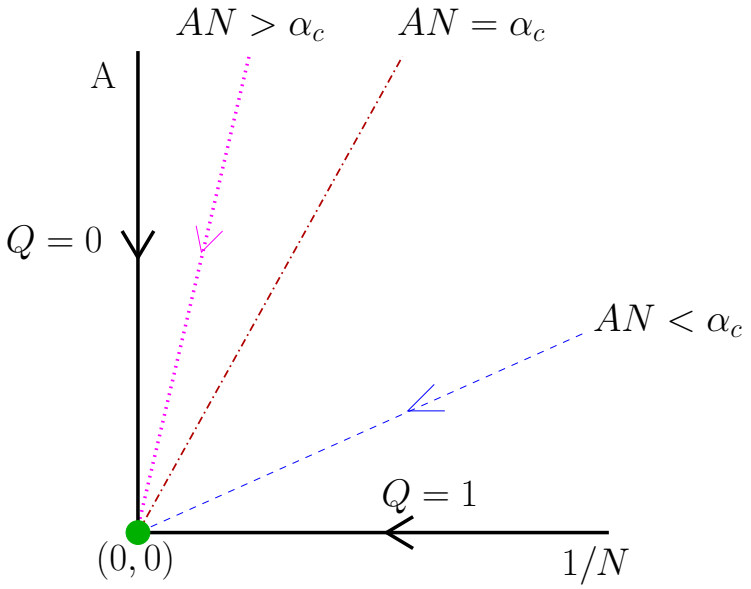


FIG. 7: Phase diagram. Various approaches to vanishing area at large-$N$ are indicated by lines with arrows. The critical value of the slope $AN = \alpha_c$ is shown as the dot-dashed line. For values of $AN \gg \alpha_c$ (the dotted line), $Q$ decays exponentially with area. For values of $AN \ll \alpha_c$ (the dashed line), $Q \approx 1$. In particular, when $A$ is reduced to 0 after taking the large-$N$ limit (*i.e.*, along $y$-axis), $Q$ vanishes. When the two limits are interchanged (*i.e.*, along $x$-axis), $Q$ becomes 1.


[3] D. J. Gross and W. Taylor, Nucl.Phys. **B400**, 181 (1993), hep-th/9301068.

[4] D. Gross and E. Witten, Phys.Rev. **D21**, 446 (1980).

[5] T. Eguchi and H. Kawai, Phys.Rev.Lett. **48**, 1063 (1982).

[6] L. D. McLerran and A. Sen, Phys.Rev. **D32**, 2794 (1985).

[7] B. Durhuus and P. Olesen, Nucl.Phys. **B184**, 461 (1981).

[8] R. Narayanan and H. Neuberger, JHEP **0712**, 066 (2007), 0711.4551.

[9] S. Datta and S. Gupta, Phys.Rev. **D82**, 114505 (2010), 1006.0938.